Reactive collisions between electrons and NO$^+$ ions: rate coefficient computations and relevance for the air plasma kinetics

O Motapon†‡, M Fifirig♯, A Florescu*\$, F O Waffeu Tamo†§, O Crumeyrolle§, G Varin-Bréant§, A Bultel¶, P Vervisch¶, J Tennyson$^+$ and I F Schneider§

† Centre for Atomic, Molecular Physics and Quantum Optics (CEPAMOQ), Faculty of Science, University of Douala, P. O. Box 8580, Douala, Cameroon

♯ Department of Chemistry, University of Bucharest, R-70900 Bucharest, Romania

* Laboratoire de Photophysique Moléculaire, Université Paris-Sud, F-91405 Orsay, France

\$ Laboratoire de Physique des Atomes, Lasers, Molécules et Surfaces, Université de Rennes I, France

§ Laboratoire de Mécanique, Physique et Géosciences, UFR Sciences et Techniques, Université du Havre, 25, rue Philippe Lebon, BP 540, 76058, Le Havre, France

¶ CORIA, Université de Rouen, Avenue de l'Université, 76800 Saint-Etienne du Rouvray, France

$^+$ Department of Physics and Astronomy, University College London, Gower Street, London WC1E 6BT, UK

Abstract. Extensive calculations of the rate coefficients for Dissociative Recombination (DR), Elastic Collisions (EC), Inelastic Collisions (IC) and Superelastic Collisions (SEC) of NO$^+$ ions on initial vibrational levels $v_i^+ = 0$ to 14 with electrons of energy between 10^{-5} eV and 10 eV have been performed, with a method based on the Multichannel Quantum Defect Theory. Comparisons of the DR rate coefficients with the plasma experimental results give a good agreement, confirming that the vibrationally excited NO$^+$ ions recombine more slowly than those in the ground state. Also, our ground state IC rate coefficients are very similar with previously computed R-matrix data. The rate coefficients have been fitted to a modified Arrhenius law, and the corresponding parameters are given, in order to facilitate the use of the reaction data in kinetical plasma modelling.

PACS numbers: 34.80, 52.20,25,72

1. Introduction

Cold plasmas containing a large number of molecules and molecular ions constitute a subject of rising scientific interest, involving more and more technological applications.

‡ Junior Associate of the Abdus Salam ICTP, Strada Costiera 11, 34014 Trieste, Italy

NO$^+$ has been proven to be one of the most important of such molecular ionic species, since it occurs in practically all air assisted processes.

During the re-entry of a spatial vehicle in the high shells of the terrestrial atmosphere, the air interacting with the vehicle's surface is compressed. This leads to a subsequent increase of its temperature and its transition to a plasma state. A detailed study of this plasma and of its interaction with the exterior wall of the spacecraft is absolutely necessary, since the corresponding material must be able to support outstanding high energy fluxes. Its kinetic description needs a good knowledge of the rate coefficients of the dominant reactions, including those between electrons and molecular ions. As for the NO$^+$ ions, which are probably the dominant ionic species in this region, their concentration is strongly affected by the *dissociative recombination*:

$$NO^+(v_i^+) + e^- \rightarrow N + O \tag{1.1}$$

but also by other related competitive processes, mainly *inelastic* $(v_f^+ > v_i^+)$ and *superelastic* $(v_f^+ < v_i^+)$ *collisions* with electrons:

$$NO^+(v_i^+) + e^- \rightarrow NO^+(v_f^+) + e^- \tag{1.2}$$

At high energy (above 10 eV), *dissociative excitation*:

$$NO^+(v_i^+) + e^- \rightarrow N^+ + O + e^-, N + O^+ + e^- \tag{1.3}$$
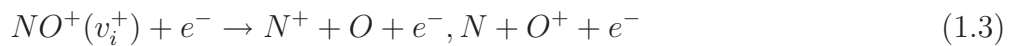
plays an important role, and at high pressure, so does *associative ionisation*:

$$N + O \rightarrow NO^+(v_f^+) + e^- \tag{1.4}$$

In the preceding equations, v_i^+ and v_f^+ stand for the initial and final vibrational quantum number of the target ion, and rotational structure was neglected.

The same elementary processes contribute to the chemistry of other discharges in N_2 and O_2 mixtures as those involved for the synthesis of nitrogen oxides, cleaning of gases exhaust resulting from combustion, plasma assisted combustion and streamer propagation.

Finally, the rate coefficients of dissociative recombination can help in the accurate estimation of the temperature seasonal variations in the lower thermosphere from the ionospheric data (Givishvili and Leshchenko 2003).

After the pioneering theoretical estimation of the DR rate coefficient by Bardsley (Bardsley 1968*a*, Bardsley 1968*b*), several measurements, using various techniques were carried out: trapped ion technique (Walls and Dunn 1974), merged electron-ion beam technique (Mul and McGowan 1979), and shock tube (Davidson and Hobson 1987).

The first elaborate DR calculations were carried out by Sun and Nakamura (1990) and Vâlcu et *al* (1998). In the former study, based on quantum chemistry computations (Nakashima *et al* 1989) and other studies (see Refs [24-30] of Sun and Nakamura (1990)) five dissociative states were considered: A' $^2\Sigma^+$, I $^2\Sigma^+$, B $^2\Pi$, L $^2\Pi$ and B' $^2\Delta$. The reaction matrix $\mathcal{K}$ was calculated within the first order approximation, and only the 10 lowest vibrational levels ($v_i^+ = 0 - 9$) were considered. This led to significantly smaller

thermal rates as compared to the most recent experimental values (Vejby-Christensen *et al* 1998, Mostefaoui *et al* 1999).

In the same way, the work by Vâlcu et *al*, which was aimed at showing the role played by rotations in the indirect recombination process through bound Rydberg states, and which used data from Giusti-Suzor and Jungen (1984) and Raoult (1987) for NO$^+$ ions, yielded smaller thermal rates than experiment. In a previous paper (Schneider *et al* 2000*a*), hereafter referred to as Paper I, *ab initio* potential curves have been calibrated from Raoult (1987) and couplings have been derived from the autoionization widths of Rabadán and Tennyson (1997) to perform a series of MQDT calculations of the dissociative recombination cross section of NO$^+$, assuming the molecular ion to be in its ground state (X$^1\Sigma^+$, $v_i^+ = 0$). In addition to the five dissociative states used by Sun and Nakamura, the highly excited $3^2\Pi$ was taken into account. All the 57 vibrational levels of the ion were considered: although many of them correspond to *closed* channels, they do contribute through the *indirect* mechanism. The results obtained were in good agreement with the low-energy experimental data, up to 3 eV, and validated the reliability of the calibrated data. Nevertheless, that work was limited to the ground vibrational state of the target ion.

Few time before, one of us and his co-workers (Rabadán and Tennyson 1999) addressed the problem of the NO$^+$ vibrational excitation (i.e. vibrational IC, eq. (1.2), $v_f^+ > v_i^+$) and, few time after (Faure and Tennyson 2001), that of its rotational excitation.

The purpose of the present work is to use the above described data set (Schneider *et al* 2000*a*) to provide a wide range of rate coefficients for reactive collisions between NO$^+$ ions and low-energy electrons, involving not only dissociative recombination and inelastic collisions, but also elastic and superelastic collisions which, to our knowledge, have not been the object of theoretical investigations for this molecular ion. This study aims to investigate the dependence of the rate coefficients on the initial vibrational level of the target and, as well, to provide data necessary to develop a kinetic model of air plasmas (Bultel *et al* 2005). The vibrational states considered are $v_i^+ = 0$ to $v_i^+ = 14$ for all the processes.

The present paper is organized as follows. The second section is concerned with a brief reminder of the theory. The third section presents the molecular data and the calculations. In the fourth section, the results are presented, discussed and compared with previously reported experimental and theoretical data. The rate coefficients of the different reactions of interest are fitted with a modified Arrhenius law in the fifth section, which is followed by the conclusion.

2. Theory

The MQDT approach (Seaton 1983, Greene and Jungen 1985, Jungen 1996, Giusti-Suzor 1980) has been shown to be a powerful method for the evaluation of the cross sections of the DR process. Although it was applied with a great success to several diatomics

like H$_2^+$ and its isotopomers (Giusti-Suzor *et al* 1983, Schneider *et al* 1991, Takagi 1993, Tanabe *et al* 1995, Schneider *et al* 1997, Amitay *et al* 1999), O$_2^+$(Guberman and Giusti-Suzor 1991, Guberman 2000), NO$^+$(Sun and Nakamura 1990, Vâlcu *et al* 1998) and triatomics like H$_3^+$ (Schneider *et al* 2000*b*, Kokoouline *et al* 2001, Kokoouline and Greene 2003), its application to vibrational transitions, mainly to superelastic collisions, is very recent (Ngassam *et al* 2003*a*).

If we aim to describe the sensitivity of the reactive electron-cation collisions on the *vibrational* levels involved, the rotational effects are known to be negligible for NO$^+$ (Vâlcu *et al* 1998), at least at first approximation. One reason for this is the weakness of the indirect process with respect to the direct one in the case of the *NO$^+$/NO* system. Since rotational structure and interactions play their role especially within the indirect mechanism - due to its resonant character - the weakness of this latter process implies that the rotational effects - if of any relevance - can be roughly restricted to the existence of the centrifugal barrier, due to the rotational excitation. But even in this latter context, rotation does not matter very much, since the target ion and the neutral are *equally* excited and, consequently, the Franck-Condon overlaps do not change in a significant way with respect to those occuring for the case of rotationally ground states.

However, this does not mean at all (Faure and Tennyson 2001) that rotational *transitions* are negligible.

Although the theoretical reminder given below - limited here to the account of the *vibrational* structure and couplings - will illustrate mainly the DR, the reader should keep in mind that the other competitive reactions - SEC, EC and IC - display quite similar features.

The DR can take place following two mechanisms/processes:

(i) the direct process where the capture takes place into a dissociative state (NO**),

$$NO^+(v_i^+) + e^- \rightarrow NO^{**} \rightarrow N + O \qquad (2.1)$$

(ii) the indirect process where the capture occurs *via* a Rydberg state NO* which is predissociated by the NO** state,

$$NO^+(v_i^+) + e^- \rightarrow NO^* \rightarrow NO^{**} \rightarrow N + O \qquad (2.2)$$
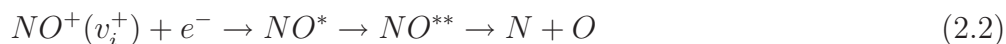
In both cases, the autoionisation is competitive with the predissociation and leads, through the reaction (1.2), to superelastic, elastic or inelastic collisions. In this work NO** and NO* represent the doubly excited and singly excited states of NO respectively.

The MQDT treatment of DR involves ionization channels (describing the electron-ion scattering) and dissociation channels (describing the atom-atom scattering). Each ionization channel consists of a Rydberg series of excited states, extrapolated above the continuum threshold — a vibrational level v^+ of the molecular ion. It is *open* if its corresponding threshold is situated *below* the total energy of the system, and *closed* in the opposite case. As for the dissociative channels, only open channels are used in the present work.

The MQDT approach is based on a description of molecular states in which only part of the electronic hamiltonian is diagonalized, within subspaces of electronic states with similar nature. We use a quasi-diabatic representation of molecular states (Sidis and Lefebvre-Brion 1971) to cope with problems due to the avoided crossings of the potential energy curves. The short-range electronic interactions between states of different subspaces are then found out in terms of an electronic coupling operator $\boldsymbol{\mathcal{V}}$ which couples the ionization channels to the dissociative channels. Starting from $\boldsymbol{\mathcal{V}}$, one builds the short-range reaction matrix $\boldsymbol{\mathcal{K}}$, solution of a Lippmann-Schwinger integro-differential equation:

$$\boldsymbol{\mathcal{K}} = \boldsymbol{\mathcal{V}} + \boldsymbol{\mathcal{V}} \frac{1}{E - H_0} \boldsymbol{\mathcal{K}} \tag{2.3}$$

H_0 being the zero order Hamiltonian associated to the molecular system, i.e. the hamiltonian operator excluding the interaction potential $\boldsymbol{\mathcal{V}}$. The effects of short-range are valid in the region of small electron-ion and nuclei-nuclei distances, that is the 'A-region' (Jungen and Atabek 1977) where the Born-Oppenheimer representation is appropriate for the description of the colliding system. There, the energy-dependence of the electronic couplings can be neglected. In the case of weak coupling, a perturbative solution of equation (2.3) can be obtained. This solution has been recently proven to be exact to second order, in the case of energy-independent electronic coupling (Ngassam *et al* 2003*b*). In the external zone, the 'B-region' (Jungen and Atabek 1977) represented by large electron-core distances, the Born-Oppenheimer model is no longer valid for the ionization channels and a close-coupling representation in terms of 'molecular ion + electron' is more appropriat e. This corresponds to a frame transformation defined by the projection coefficients:

$$\mathcal{C}_{lv^+,\Lambda\alpha} = \sum_v U^\Lambda_{lv,\alpha} \langle \chi_{v^+} | \cos(\pi\mu^\Lambda_l(R) + \eta^\Lambda_\alpha) | \chi^\Lambda_v \rangle \tag{2.4}$$

$$\mathcal{C}_{d_j,\Lambda\alpha} = U^\Lambda_{d_j\alpha} \cos \eta^\Lambda_\alpha \tag{2.5}$$

$$\mathcal{S}_{lv^+,\Lambda\alpha} = \sum_v U^\Lambda_{lv,\alpha} \langle \chi_{v^+} | \sin(\pi\mu^\Lambda_l(R) + \eta^\Lambda_\alpha) | \chi^\Lambda_v \rangle \tag{2.6}$$

$$\mathcal{S}_{d_j,\Lambda\alpha} = U^\Lambda_{d_j\alpha} \sin \eta^\Lambda_\alpha \tag{2.7}$$

In the preceding formulae, χ_{v^+} is a vibrational wavefunction of the molecular ion, and χ_v is a vibrational wavefunction adapted to the interaction (A) region. The index α denotes the eigenchannels built through the *diagonalization* of the reaction matrix $\boldsymbol{\mathcal{K}}$ — equation (2.3)— and $U_{lv,\alpha}$ and η^Λ_α are related to the corresponding eigenvectors and eigenvalues. The projection coefficients shown in (2.4) include the two types of couplings controlling the process: the *electronic* coupling, expressed by the elements of the matrices $\boldsymbol{U}$ and $\boldsymbol{\eta}$, and the *non-adiabatic* coupling between the ionization channels, expressed by the matrix elements involving the quantum defect μ^Λ_l. This latter interaction is favored by the variation of the quantum defect with the internuclear distance R. The matrices $\boldsymbol{\mathcal{C}}$

and $\boldsymbol{S}$ with elements (2.4) and (2.5) are the building blocks of the 'generalized' scattering matrix $\boldsymbol{X}$:

$$\boldsymbol{X} = \frac{\boldsymbol{C} + i\boldsymbol{S}}{\boldsymbol{C} - i\boldsymbol{S}} \tag{2.8}$$

whereas the 'proper' scattering matrix, restricted to the *open* channels, is given by (Seaton 1983):

$$\boldsymbol{S} = \boldsymbol{X}_{oo} - \boldsymbol{X}_{oc}\frac{1}{\boldsymbol{X}_{cc} - \exp(-\mathrm{i}2\pi\boldsymbol{\nu})}\boldsymbol{X}_{co} \tag{2.9}$$

It is obtained from the sub-matrices $\boldsymbol{X}$ involving the lines and columns associated with the open (o) and closed (c) channels, and a further diagonal matrix $\boldsymbol{\nu}$ formed with the effective quantum numbers $\nu_{v^+} = [2(E_{v^+} - E)]^{-1/2}$ (in atomic units) associated with each vibrational threshold E_{v^+} of the ion situated *above* the current energy E. For a molecular ion initially in the level v_i^+ and recombining with an electron of energy ε, the cross section of capture into *all* the dissociative states d_j of the same symmetry Γ is given by:

$$\sigma^{\Gamma}_{\mathrm{diss} \leftarrow v_i^+} = \frac{\pi}{2} \cdot \frac{\rho^{\Gamma}}{2} \cdot \frac{1}{\varepsilon} \cdot \sum_j \sum_l |S^{\Gamma}_{d_j \leftarrow lv_i^+}|^2 \tag{2.10}$$

Here Γ refers to the electronic symmetry of the neutral species ($^2\Sigma^+$, $^2\Pi$ and $^2\Delta$ in the present study) and ρ^{Γ} is the ratio between the multiplicities of the neutral system and the ion. One has to perform the MQDT calculation for each group of dissociative states of symmetry Γ, and the sum over the resulting cross sections is the total DR cross section:

$$\sigma_{\mathrm{diss} \leftarrow v_i^+} = \sum_{\Gamma} \sigma^{\Gamma}_{\mathrm{diss} \leftarrow v_i^+} \tag{2.11}$$

In a similar way, the cross section for a vibrational transition of a molecular ion from the initial level v_i^+ to the final level v_f is:

$$\sigma^{\Gamma}_{v_f^+ \leftarrow v_i^+} = \frac{\pi}{2} \cdot \frac{\rho^{\Gamma}}{2} \cdot \frac{1}{\varepsilon} \cdot \sum_{l,l'} |S^{\Gamma}_{l'v_f^+ \leftarrow lv_i^+}|^2 \tag{2.12}$$

and the total cross section for this vibrational transition is:

$$\sigma_{v_f^+ \leftarrow v_i^+} = \sum_{\Gamma} \sigma^{\Gamma}_{v_f^+ \leftarrow v_i^+} \tag{2.13}$$

3. Molecular data and calculations

In Paper I, we had used the *ab initio* potential curves produced by MQDT interpretation of spectroscopic data (Raoult 1987) from high-precision spectroscopic measurements (Dressler and Miescher 1981) to build 'calibrated' curves. The calibration consisted of using all the data available to put the minima of the curves in coincidence with the spectroscopic data, and then to derive the asymptotic limit. The data are plotted
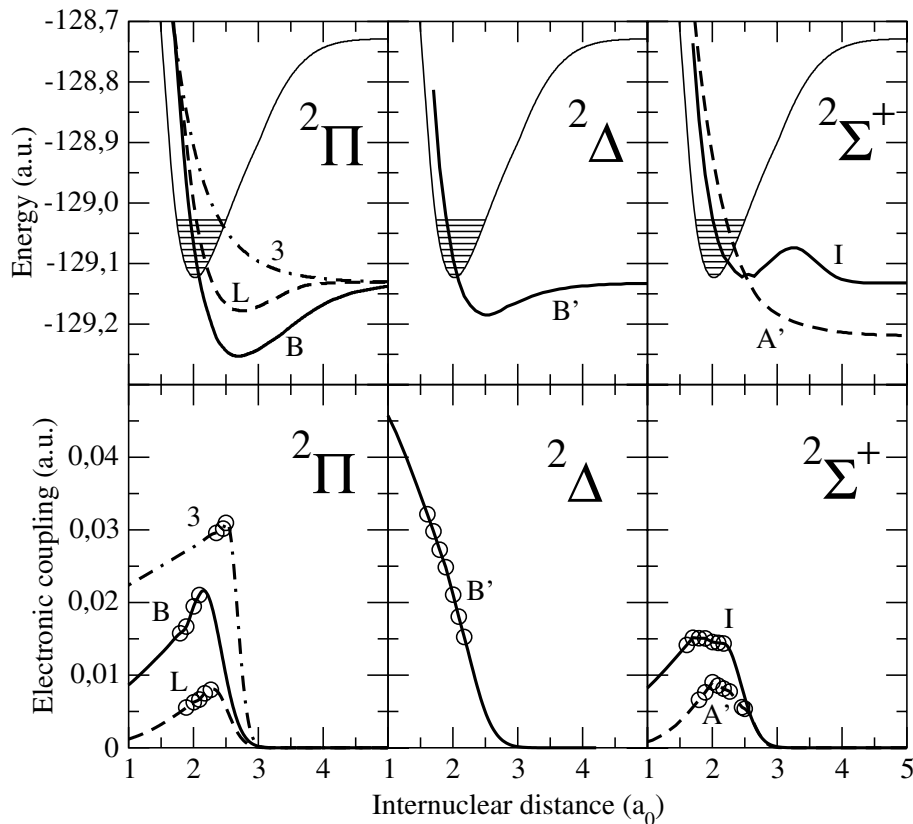
Figure 1. Quasi-diabatic representation of NO super-excited states of all the relevant symmetries (from Schneider *et al* (2000*a*)). Some vibrational states of the NO$^+$ground electronic state (fine continuous curve) are represented as black horizontal lines. The circles label values of the electronic couplings computed by the R-matrix method (Rabadán and Tennyson 1996, Rabadán and Tennyson 1997)

in Figure 1 for all the symmetries. Figure 1 also displays the electronic couplings $V_{d_j}(R)$, derived from R-matrix calculations (Rabadán and Tennyson 1996, Rabadán and Tennyson 1997, Rabadán and Tennyson 1998, Tennyson 2000) of autoionization widths $\Gamma_{d_j}(R)$ by

$$V_{d_j}^\Lambda(R) = [\Gamma_{d_j}^\Lambda(R)/(2\pi)]^{1/2} \tag{3.1}$$

It can be seen that most of the interaction takes place at distances $R \leq 3$ a.u. Using the set of molecular data described above, we have performed a series of MQDT calculations of the cross sections of DR, EC, SEC, and IC, with the molecular ion in different vibrational levels ($v_i^+ = 0$ to 14) of its ground electronic state. This is aimed at evaluating the relative contributions of the vibrationally excited states of NO$^+$ on its dissociative recombination, and the role of autoionization (SEC, EC and IC) on the dynamics of NO$^+$ in interaction with low-energy electrons. The rotational structure, as stated above, is not considered, nor are spin-orbit effects. The cross sections are calculated separately for each symmetry (involving all the relevant dissociative states within the symmetry) and are summed to give the total cross section. The energy range
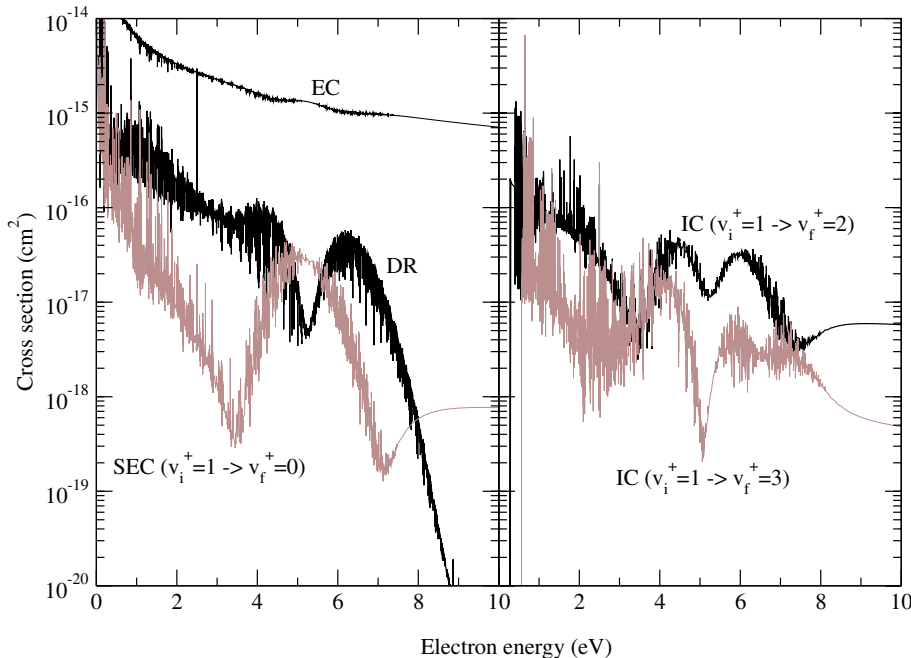
Figure 2. Total cross sections for Dissociative Recombination, Elastic Collisions, Superelastic Collisions and Inelastic Collisions of $NO^+(X\ ^1\Sigma^+)$, from the initial vibrational state $v_i^+ = 1$. The total cross section is the sum of all the contributions from all the symmetries and, within each symmetry, from all the relevant dissociative states.

of the incident electron is 0.01 meV–10 eV, in steps of 0.01 meV. As in Paper I, for each dissociative channel available, we have considered its interaction with only one Rydberg series: $p\pi$ for the $^2\Pi$ states, $p\sigma$ for the A' $^2\Sigma^+$, $s\sigma$ for the I' $^2\Sigma^+$ and $d\delta$ for the B' $^2\Delta$ states; both direct and indirect mechanisms have been accounted for.

One can doubt about the sufficiency of the electronic states involved in the present series of computations - Figure 1. Further excited dissociative states certainly exist within each symmetry. However, exploratory R-matrix calculations have shown that, for the $^2\Pi$ symmetry, the potential curve of the next higher dissociative state should cross that of the ion above the highest initial vibrational level of the target ion considered in this article, $v_i^+ = 14$. As for the other symmetries, the interactions of the next higher dissociative states with the electron-ion continuum seem to be weak. On the other hand, even if the very highly excited vibrational states ($v^+ > 14$) may generate strong couplings between the ionization continuum and the high dissociative states, the relative weakness of the indirect process should prevent these latter states to play a major role. The situation would certainly change if the ion target would be furthermore vibrationally excited ($v_i^+ > 14$), in which case further *ab-initio* computations of states and couplings would be required.
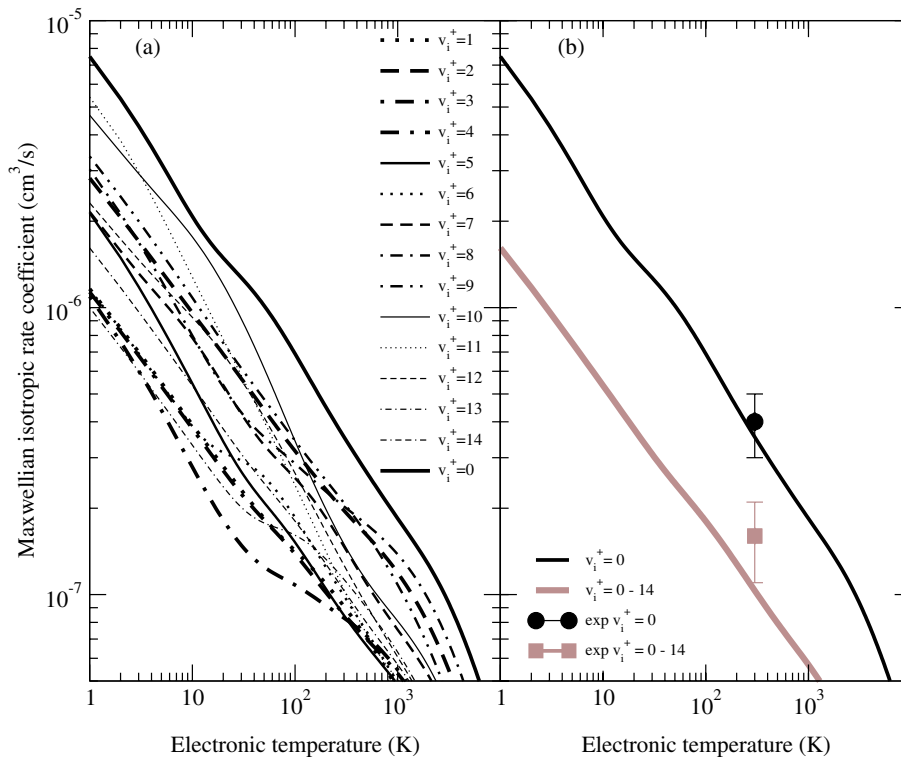
Figure 3. (a) Computed Maxwellian isotropic rate coefficient of DR of NO$^+$(X $^1\Sigma^+$) initially in its first 15 vibrational levels, as a function of the temperature of the incident electrons. (b) Comparison with three experimental results: ground state using storage ring (Vejby-Christensen *et al* 1998) and flowing afterglow Langmuir probe (Mostefaoui *et al* 1999) in black, and mixture of vibrational states (Mostefaoui *et al* 1999) in grey. In the case $v_i^+ = 0$, the two experimental results are very close to each other: $4 \times 10^{-7} cm^3/s$ (Vejby-Christensen *et al* 1998) and $(4 \pm 1) \times 10^{-7} cm^3/s$ (Mostefaoui *et al* 1999).

4. Results and Discussion

We start this section by an illustration of the cross sections for all the processes (Figure 2) for the case of the initial vibrational level $v_i^+ = 1$, as an example, before presenting the rate coefficients. The cross sections exhibit structures due to the indirect process, i.e. the temporary capture on Rydberg states of the NO molecule. They present one or several broad peaks separated by pronounced dips which are due, in general, to the variation with energy of the overlap of the vibrational and the dissociative wavefunctions (Franck-Condon effects). If we restrict ourselves to the direct process, there is one single vibrational wave function involved in the overlap integrals for DR and EC, and two vibrational wave functions in the case of SEC and IC (Nakashima *et al* 1987); this explains the larger number of dips observed for SEC and IC, related to the nodes of the vibrational wave functions involved.

The peak around 6 eV in DR is similar to the one put in evidence by the ASTRID storage ring for the DR from the ground $v_i^+ = 0$ state, and which was almost entirely
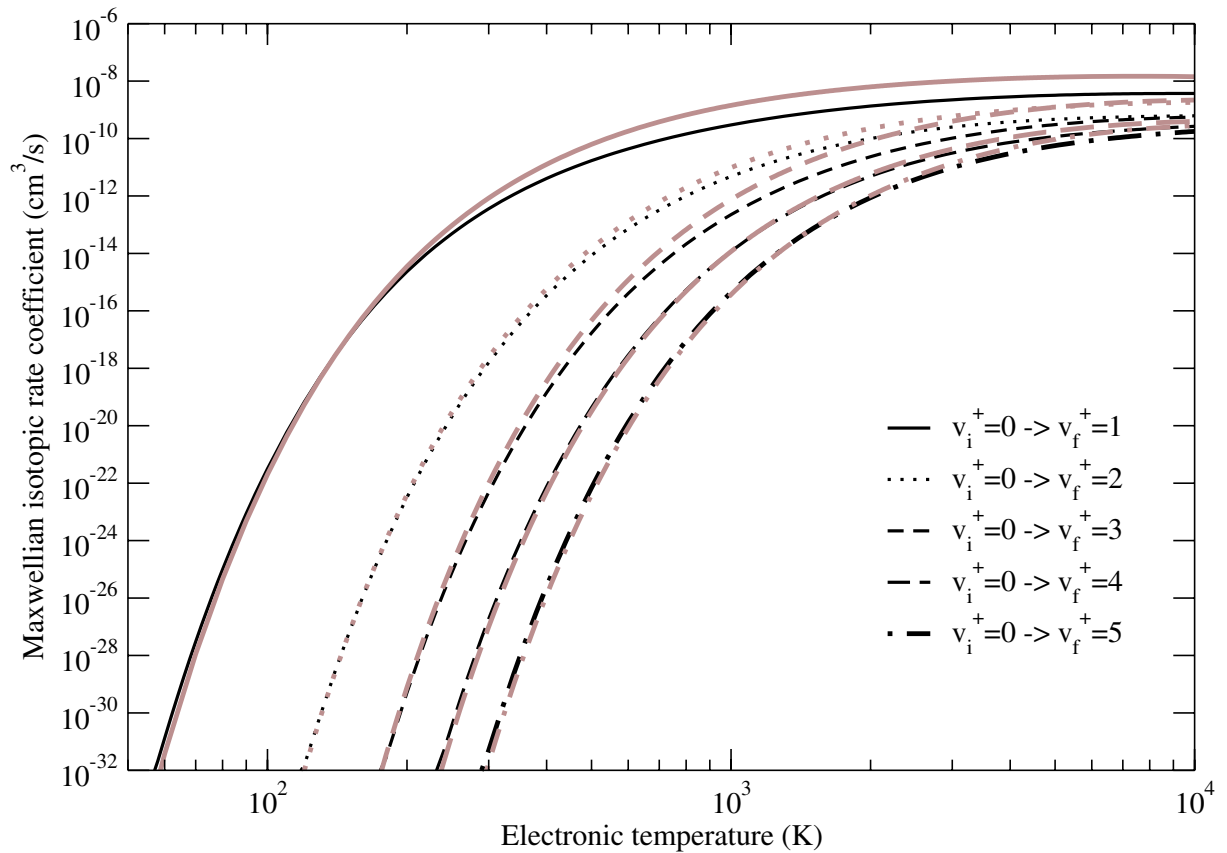
Figure 4. Comparison of Maxwellian isotropic rate coefficients obtained in this work with those obtained from an R-matrix-based calculation of the electron impact vibrational excitation (Rabadán and Tennyson 1999) for the transitions from $v_i^+ = 0$ to $v_f^+ = 1$ to 5: black lines: this work; grey lines: Rabadán and Tennyson (1999).

found to be due to the 3 $^2\Pi$ state. The EC cross sections present a global E^{-1} behavior, and are about two to three orders of magnitude greater than those for DR, SEC and IC. The cross sections for superelastic and inelastic collisions tend to a plateau for electron energies exceeding 8 eV, due to the fall-off of the DR cross sections which prevents from a flux loss to the dissociation channels. Those for inelastic collisions from a given initial vibrational state are non-zero only when the electron energy exceeds the excitation threshold, and are of the same order of magnitude as those for the inverse SEC cross sections.

Maxwellian isotropic rate coefficients computed for the DR of NO$^+$ in its first 15 vibrational levels, i.e. $v_i^+ = 0$ to 14, are represented in Figure 3a. One may notice that, for any temperature, the rate coefficients for different initial vibrational levels hold within an order of magnitude, and that the vibrationally relaxed ions recombine faster than the excited ones. Comparison has been made with three experiments for two situations: $v_i^+ = 0$ on one hand, and a mixture of vibrationally excited states at $T = 300\ K$ on the other hand. The results are represented in Figure 3b. The first experiment, based on ion storage ring technique (Vejby-Christensen *et al* 1998),
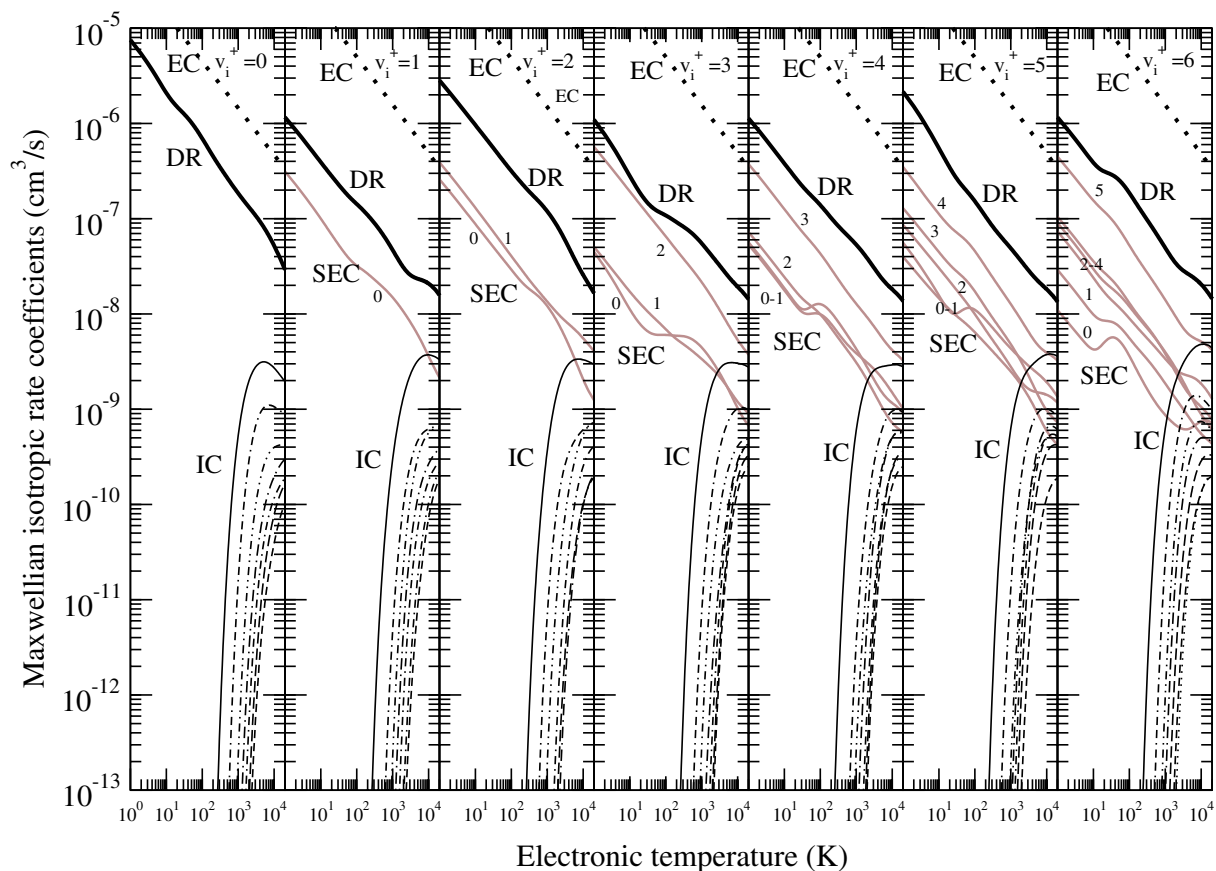
Figure 5. Rate Coefficients for Dissociative Recombination (thick full curves), Elastic Collisions (thick dotted curves), Superelastic Collisions (full grey curves) and Inelastic Collisions (thin black curves) of $NO^+(X\ ^1\Sigma^+)$, from the initial vibrational states $v_i^+ = 0-6$. For SEC, the vibrational quantum number of the final states v_f^+ is indicated near the curve, wherever it is possible. The notation $v_f^+ - v_f^{+'}$, with $v_f^+ < v_f^{+'}$, is used when the curves are too close. For IC, the curves are plotted in the natural order for the first seven transitions.

insured an entirely vibrationally relaxed ion population. Starting from the measured cross sections, the thermal $(300\ K)$ rate was calculated by numerical integration. In the second experiment, a flowing afterglow Langmuir probe-mass apparatus (Mostefaoui *et al* 1999) was used, with NO as parent gas; justifying the assumption that NO^+ is almost entirely in its ground vibrational state. The rate coefficient derived at $T = 300\ K$ are identical, within the error bar, for the two experiments: $((4 \pm 1) \times 10^{-7} cm^3/s$ and $4 \times 10^{-7} cm^3/s$ respectively. The third experiment used the same experimental setup with the second one, with N_2 and O_2 as parent gases.! It was not possible, in this case, to obtain totally vibrationally relaxed NO^+ ions, but the population distribution of the different vibrational levels of NO^+ ions formed have been measured, as well as the DR rate coefficients of the so-obtained mixture of ions at $T = 300\ K$.

Using the vibrational population distribution of the latter experiment (Mostefaoui *et al* 1999), we obtain a weighted rate coefficient corresponding to the experimental
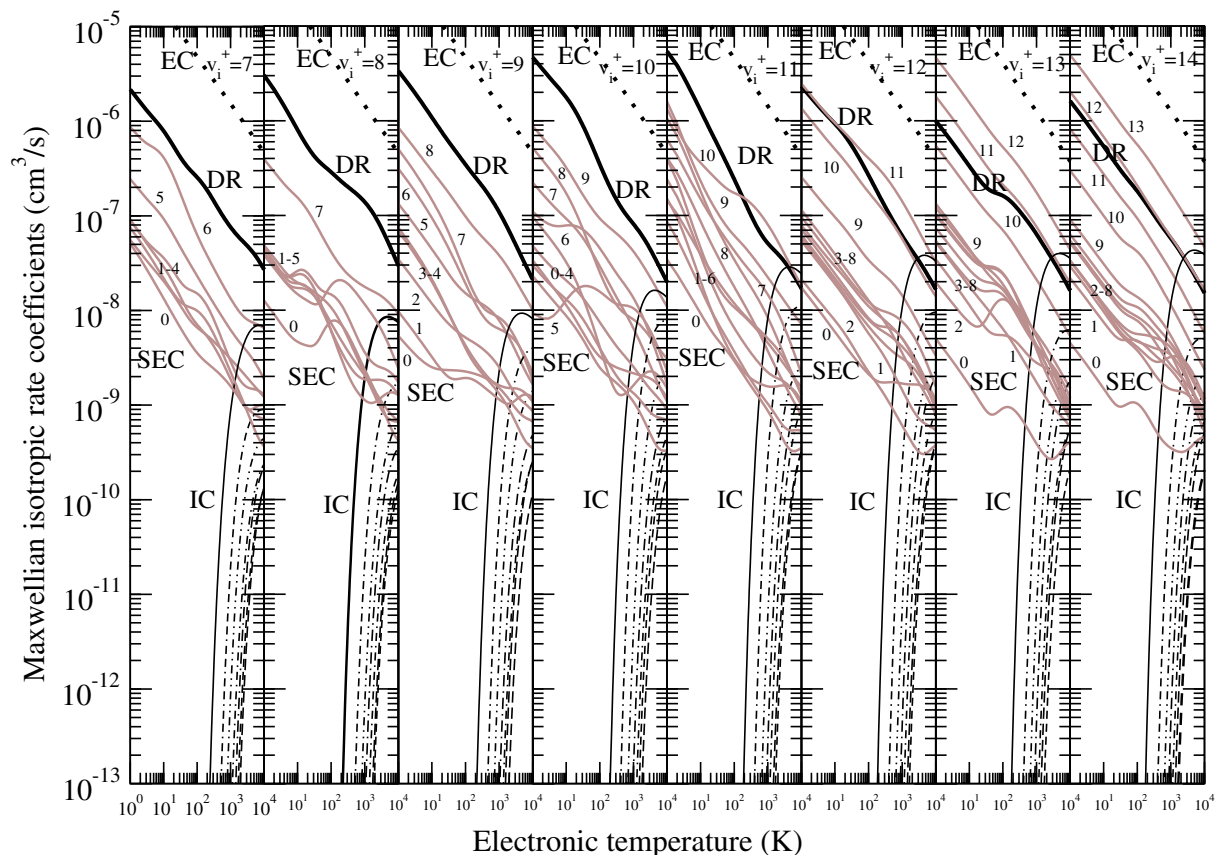
Figure 6. Same as figure 4 for $v_i^+ = 7 - 14$

mixture of vibrational states. The results represented in Figure 3b show quite a good agreement with the experiment, at the temperature $T = 300$ K, thus confirming that for the excited vibrational levels the DR rate coefficient is lower than that for $v_i^+ = 0$.

On the other hand, our electron impact vibrational excitation Maxwellian isotropic rates agree very well with those obtained from an R-matrix calculation (Rabadán and Tennyson 1999) for the transitions from $v_i^+ = 0$ to $v_f^+ = 1$ to 5, as shown in Figure 4.

In Figures 5 and 6 , we represent the rate coefficients of all the processes for $v_i^+ = 0$ to 6, and $v_i^+ = 7$ to 14, respectively. It can be seen on these figures that the rate coefficient for elastic collisions α_{EC} is practically independent of v_i^+, in contrast to the rate coefficients for DR (α_{DR}) and SEC (α_{SEC}). It can be also observed that the DR rate coefficients, which are greater than the SEC rates at low v_i^+, are dominated by the first superelastic transitions at the high values of v_i^+. The IC rate coefficients increase with v_i^+. Moreover, whereas α_{EC} scales globally as a power of the temperature, α_{DR} and α_{SEC} have a variable temperature dependence, due to the broad peaks observed on the corresponding cross sections.

5. Fitting of the reaction rate coefficients

In order to facilitate their use, the isotropic Maxwellian rate coefficients of the reactions investigated in this work for NO$^+$ ions have been fitted to a modified Arrhenius law, i.e:

$$\alpha_P(T_e, v_i^+, v_f^+) = A T_e^{-\gamma} e^{-\theta/T_e} \tag{5.1}$$

where the subscript P indicates the process, T_e is the electron temperature, v_i^+ and v_f^+ are the initial and final vibrational quantum numbers of the target ion.

Naturally, the parameters A, γ and θ depend only on v_i^+ for DR and EC, whereas they also depend on v_f^+ for the other reactions. These parameters have been calculated for the temperature range $2000 \leq T_e \leq 10000 \ K$ for which NO$^+$ plays a major role in the thermal plasmas.

5.1. Dissociative recombination

The fitting of the DR rate coefficients for each v_i^+ gives $\alpha_{DR}(T_e, v_i^+)$. The *global* rate coefficient is obtained by averaging the $\alpha_{DR}(T_e, v_i^+)$ on all possible vibrational levels assuming they are in Boltzmann equilibrium according to T_e, i.e:

$$\alpha_{DR}(T_e) = \sum_{v_i^+} \alpha_{DR}(T_e, v_i^+) \frac{g(v_i^+) e^{-E_{v_i^+}/k_B T_e}}{\sum_{v_i^+} g(v_i^+) e^{-E_{v_i^+}/k_B T_e}} \tag{5.2}$$

where $g(v_i^+)$ is the statistical weight of the vibrational level v_i^+.

Proceeding as indicated above, we have found for DR the values of A, γ and θ reported on Table 1 as well as the global rate coefficient

$$\alpha_{DR}(T_e) = 1.610 \times 10^{-4} \, T_e^{-0.929} \, e^{-\frac{377.36}{T_e}} \qquad cm^3 s^{-1} \tag{5.3}$$

We have to recall that the results displayed in section 4 have been calculated neglecting the rotational structure of the molecular ion, i.e. putting J equal to 0 and $g(v_i^+) = 1$ for all v_i^+: any comparison between the previous rate coefficient and that derived from experience must be performed in the light of this limitation. Taking into account the rotational excitation and assuming a same rate coefficient whatever the value of J for a given vibrational level (which is the consequence on rate coefficients of the fact that rotation do not play a role in the DR of NO$^+$), the global rate coefficient is then :

$$\alpha'_{DR}(T_e) = 1.658 \times 10^{-4} \, T_e^{-0.933} \, e^{-\frac{377.68}{T_e}} \qquad cm^3 s^{-1} \tag{5.4}$$

which is quite close to $\alpha_{DR}(T_e)$ (Eq.5.3). From a theoretical point of view, a comparison should be made between experimental results where they exist and the rate coefficient (5.4) rather than with $\alpha_{DR}(T_e)$, if the rotation is sufficiently excited.

5.2. Superelastic and inelastic collisions

Tables 2 to 4 contain the parameters A, γ and θ for SEC, EC and IC, as a function of v_i^+ and v_f^+, where v_i^+ and v_f^+ have been chosen less than 6 in order to limit the size of the tables to be presented. At thermodynamic equilibrium, the two processes

$$NO^+(v_i^+) + e^- \rightarrow NO^+(v_f^+) + e^- \tag{5.5}$$

and

$$NO^+(v_f^+) + e^- \rightarrow NO^+(v_i^+) + e^- \tag{5.6}$$
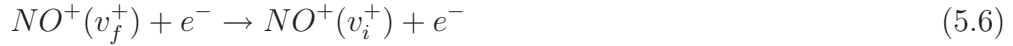
with reaction rates $\alpha_{i\rightarrow f}$ and $\alpha_{f\rightarrow i}$ are perfectly balanced, due to the microreversibility. This has been verified by parametrizing the equilibrium constant

$$K_{eq}(T_e, v_i^+, v_f^+) = \frac{\alpha_{f\rightarrow i}}{\alpha_{i\rightarrow f}} = \frac{g(v_i^+)}{g(v_f^+)} e^{-(E_{v_i^+} - E_{v_f^+})/k_B T_e} \tag{5.7}$$

in the form

$$K_{eq}(T_e, v_i^+, v_f^+) = A_{eq} T_e^{-\gamma_{eq}} e^{-\theta_{eq}/T_e} \tag{5.8}$$

where $A_{eq} = A_{f\rightarrow i}/A_{i\rightarrow f}$, $\gamma_{eq} = \gamma_{f\rightarrow i} - \gamma_{i\rightarrow f}$ and $\theta_{eq} = \theta_{f\rightarrow i} - \theta_{i\rightarrow f}$. The parameters obtained for the equilibrium constant K_{eq} are represented on Table 5 where it can be seen that γ_{eq} is close to 0, such that the temperature dependence of K_{eq} is contained mainly in the exponential factor. In addition, the fact that θ_{eq} is quite close to $(E_{v_i^+} - E_{v_f^+})/k_B$ and that A_{eq} is close to 1 validate the fit of these rate coefficients.

5.3. Elastic collisions

For elastic collisions, the parameters A, γ and θ derived from the fit of $\alpha_{EC}(T_e, v_i^+)$ are represented in Table 6. Assuming that the rotational effects are negligible in the elastic collisions as in the case of DR, the rates are averaged like the $\alpha'_{DR}(T_e, v_i^+)$ in equation (5.4) to obtain a global EC rate coefficient in the form:

$$\alpha_{EC}(T_e) = 5.980 \times 10^{-5} T_e^{-0.524} e^{-\frac{126.81}{T_e}} \qquad cm^3 s^{-1} \tag{5.9}$$

6. Conclusions

The cross sections and rate coefficients for reactive collisions (Dissociative Recombination, Elastic, Inelastic and Superelastic Collisions) between electrons and NO^+ ions, for the first 15 vibrational levels of the ground NO^+ ($X^1\Sigma^+$) electronic state have been computed. The energy range considered is $10^{-5} - 10 \ eV$. The comparison with experiment, for a mixture of vibrational states at T=300 K, gives a good agreement, thus confirming that NO^+ions recombine less efficiently in vibrationally excited states than in the ground state.

The rate coefficients obtained have been fitted to a modified Arrhenius law, and the parameters generated in the temperature range $2000 \leq T \leq 10000 \ K$ facilitate the

v^+	A	γ	θ	v^+	A	γ	θ
0	8.486×10^{-5}	0.793	859.99	8	1.071×10^{-4}	0.884	546.20
1	3.958×10^{-8}	0.0757	-661.83	9	1.445×10^{-5}	0.710	-67.49
2	1.664×10^{-5}	0.704	-39.13	10	2.145×10^{-5}	0.755	357.59
3	6.355×10^{-7}	0.383	-282.98	11	1.095×10^{-5}	0.695	703.00
4	2.970×10^{-7}	0.311	-632.21	12	8.897×10^{-6}	0.678	406.55
5	2.666×10^{-7}	0.297	-472.45	13	8.483×10^{-6}	0.677	276.17
6	3.623×10^{-7}	0.311	-1.109	14	8.149×10^{-6}	0.679	303.70
7	1.451×10^{-5}	0.672	852.89				

Table 1. Parameters A, γ and θ for the dissociative recombination, $\alpha_{DR}(T_e, v_i^+)$ being expressed in $cm^3 s^{-1}$.

v_i^+	v_f^+ 0	1	2	3	4	5
0	4.011×10^{-5}	4.964×10^{-6}	1.844×10^{-5}	1.812×10^{-6}	7.777×10^{-8}	5.859×10^{-7}
1	9.229×10^{-6}	6.437×10^{-5}	1.744×10^{-7}	2.957×10^{-7}	5.292×10^{-7}	2.575×10^{-7}
2	1.862×10^{-5}	2.360×10^{-7}	4.837×10^{-5}	5.651×10^{-7}	8.495×10^{-9}	1.172×10^{-9}
3	2.284×10^{-6}	3.064×10^{-7}	1.362×10^{-6}	5.686×10^{-5}	1.932×10^{-7}	6.729×10^{-8}
4	7.187×10^{-8}	5.386×10^{-7}	8.653×10^{-9}	1.933×10^{-7}	6.255×10^{-5}	2.421×10^{-8}
5	6.873×10^{-7}	2.733×10^{-7}	1.050×10^{-9}	6.724×10^{-8}	2.091×10^{-8}	6.460×10^{-5}

Table 2. Parameters A for superelastic and inelastic collisions, $\alpha(T_e, v_i^+, v_f^+)$ being expressed in $cm^3 s^{-1}$.

v_i^+	v_f^+ 0	1	2	3	4	5
0	0.484	0.773	0.982	0.802	0.514	0.747
1	0.844	0.530	0.373	0.594	0.629	0.612
2	0.983	0.405	0.502	0.517	0.231	-0.012
3	0.831	0.598	0.603	0.518	0.420	0.384
4	0.507	0.631	0.233	0.420	0.527	0.211
5	0.763	0.618	-0.024	0.384	0.196	0.531

Table 3. Parameters γ for superelastic and inelastic collisions.

v_i^+		v_f^+ 0	1	2	3	4	5
	0	-34.20	3890.5	7197.7	10398.5	12562.8	16479.4
	1	706.8	57.59	4035.3	6961.8	10469.0	12452.1
	2	563.9	152.4	33.31	3832.3	5216.8	8789.1
	3	538.7	423.3	-84.99	40.11	2916.2	6516.6
	4	-550.6	727.6	-1234	-287.1	69.01	1870.5
	5	330.5	-420.0	-856.4	154.1	-1153	72.08

Table 4. Characteristic temperature $\theta(K)$ for superelastic, elastic and inelastic collisions.

v_i^+	v_f^+	A_{eq}	γ_{eq}	θ_{eq}	$(E_{v_i^+} - E_{v_f^+})/k_B$
1	0	0.538	-0.071	3183.7	3339.1
2	0	0.990	-0.001	6633.8	6639.7
3	0	0.793	-0.029	9859.8	9892.3
4	0	1.082	0.007	13113.	13097.
5	0	0.852	-0.016	16149.	16253.
2	1	0.739	-0.032	3882.9	3300.7
3	1	0.965	-0.004	6538.5	6553.2
4	1	0.983	-0.002	9741.4	9757.4
5	1	0.942	-0.006	12872.	12914.
3	2	0.415	-0.086	3917.3	3252.5
4	2	0.982	-0.002	6450.8	6556.7
5	2	1.116	0.012	9645.5	9612.8
4	3	0.999	0.	3203.3	3204.2
5	3	1.001	0.	6362.5	6360.3
5	4	1.158	0.015	3023.5	3156.1

Table 5. Parameters A_{eq}, γ_{eq} and θ_{eq} allowing the calculation of K_{eq} from $\alpha_{i \longrightarrow f}$ and $\alpha_{f \longrightarrow i}$. The last column contains the remaining parameter of equation (5.7), $g(v_i^+)/g(v_f^+)$ being equal to 1.

use of these results in air plasma kinetic models. Moreover, the fact that we have now the rate coefficients given for each vibrational level allows a complete calculation of the vibrational distribution of NO⁺ under chemical non-equilibrium conditions. That is particularly important since the vibrational characteristic time scale is often long, and since NO⁺ is the major ionic species in N_2/ O_2 mixtures and air discharges.

v^+	A	α	θ	v	A	α	θ
0	4.011×10^{-5}	0.484	-34.20	8	4.013×10^{-5}	0.486	-37.15
1	6.437×10^{-5}	0.530	57.59	9	4.698×10^{-5}	0.502	7.05
2	4.837×10^{-5}	0.502	33.31	10	4.713×10^{-5}	0.506	-24.11
3	5.686×10^{-5}	0.518	40.11	11	5.157×10^{-5}	0.522	-35.50
4	6.255×10^{-5}	0.527	69.01	12	4.927×10^{-5}	0.525	-18.69
5	6.460×10^{-5}	0.531	72.08	13	4.578×10^{-5}	0.522	-17.97
6	6.682×10^{-5}	0.536	62.86	14	4.534×10^{-5}	0.522	-42.81
7	5.013×10^{-5}	0.508	-34.68				

Table 6. Parameters A, γ and θ for the elastic collisions, $\alpha_{EC}(T_e, v_i^+)$ being expressed in $cm^3 s^{-1}$.

References

Amitay Z, Baer A, Dahan M, Levin J, Vager Z, Zajfman D, Knoll L, Lange M, Schwalm D, Wester R, Wolf A, Schneider I F, and Suzor-Weiner A 1999 *Phys. Rev. A* **60** 3769
Bardsley J N 1968*a J. Phys. B: At. Mol. Phys.* **1** 349
Bardsley J N 1968*b J. Phys. B: At. Mol. Phys.* **1** 365
Bultel A et *al* 2005 *In preparation*
Davidson D F and Hobson R M 1987 *J. Phys. B: At. Mol. Phys.* **20** 5753
Dressler K and Miescher E 1981 *J. Chem. Phys.* **75** 4310
Faure A and Tennyson J 2001 *Month. Not. R: Astr. Soc.* **325** 443

Giusti-Suzor A 1980 *J. Phys. B: At. Mol. Phys.* **13** 3867

Giusti-Suzor A, Bardsley J. N and Derkits C 1983 *Phys. Rev. A* **28** 682-691

Giusti-Suzor A and Jungen Ch 1984 *J. Chem. Phys.* **80** 986

Givishvili G V and Leshchenko L N *Int.Journ.Geomagn.Aeron.***4**, 153

Greene C H and Jungen C 1985 *Adv. At. Mol. Phys.* **21** 51

Guberman S L 1994 *Phys. Rev. A* **49** R4277

Guberman 2000 *in* M Larsson, J B A Mitchell and I F Schneider, eds, 'Dissociative Recombination: Theory, Experiment and Applications IV' World Scientific Singapore p. 111

Guberman S L and Giusti-Suzor A 1991 *J. Chem. Phys.* **95** 2602,

Jungen C 1996, ed, 'Molecular Applications of Quantum Defect Theory' Institute of Physics Publishing Bristol

Jungen C and Atabek O 1977 *J. Chem. Phys.* **66** 5584

Kokoouline V, Greene C H and Esry B D 2001 *Nature* **412** 891

Kokoouline V and Greene C H 2003 *Phys. Rev. A* **68** 012703

Mostefaoui T, Laubé S, Gautier G, Rebrion-Rowe C, Rowe B R and Mitchell J. B A 1999 *J. Phys. B: At. Mol. Opt. Phys.* **32** 5247

Mul P M and McGowan J W 1979 *J. Phys. B: At. Mol. Phys.* **12** 1591

Nakashima K, Takagi H and Nakamura H 1987 *J. Chem. Phys.* **86** 726

Nakashima K, Nakamura H, Achiba Y and Kimura K 1989 *J. Chem. Phys.* **91** 1603

Ngassam V, Motapon O, Florescu A, Pichl L, Schneider I F and Suzor-Weiner A 2003*a Phys. Rev. A* **68** 032704

Ngassam V, Florescu A, Pichl L, Schneider I F, Motapon O, and Suzor-Weiner A 2003*b Eur. Phys. J. D* **26** 165

Rabadán I and Tennyson J 1996 *J. Phys. B: At. Mol. Opt. Phys.* **29** 3747

Rabadán I and Tennyson J 1997 *J. Phys. B: At. Mol. Opt. Phys.* **30** 1975

Rabadán I and Tennyson J 1998 *J. Phys. B: At. Mol. Opt. Phys.* **31** 4485

Rabadán I and Tennyson J 1999 *J. Phys. B: At. Mol. Opt. Phys.* **32** 4753

Raoult M 1987 *J. Chem. Phys.* **87** 4736

Schneider I F, Strömholm C, Carata L, Urbain X, Larsson M and Suzor-Weiner A 1997 *J. Phys. B: At. Mol. Opt. Phys.* **30** 2687

Schneider I F, Dulieu O and Giusti-Suzor A 1991 *J. Phys. B: At. Mol. Phys.* **24** L289

Schneider I F, Rabadán, Carata L, Andersen L H, Suzor-Weiner A and Tennyson J 2000*a J. Phys. B: At. Mol. Opt.Phys.***33** 4849

Schneider I F, Orel A E and Suzor-Weiner A 2000*b Phys. Rev. Lett.* **85** 3785

Seaton M J 1983 *Rept. Prog. Phys.* **46** 167

Sidis V and Lefebvre-Brion H 1971*J. Phys. B* **4** 1040

Sun H and Nakamura H 1990 *J. Chem. Phys.* **93** 6491

Takagi H 1993 *J. Phys. B: At. Mol. Opt. Phys.* **26** 4815

Tanabe T, Katayama I, Kamegaya H, Chida K, Arakaki Y, Watanabe T, Yoshizawa M, Saito M, Haruyama Y, Hosono K, Hatanaka K, Honma T, Noda K, Ohtani S and Takagi H 1995 *Phys. Rev. Lett.* **75** 1066

Tennyson 2000 *in* M Larsson, J B A. Mitchell and I F Schneider, eds, 'Dissociative Recombination: Theory, Experiment and Applications IV' World Scientific Singapore p. 121

Vâlcu B, Schneider I F, Raoult M, Strömholm C, Larsson M and Suzor-Weiner A 1998 *European Physical Journal D* **1** 71

Vejby-Christensen L, Kella D, Pedersen H B and Andersen L H 1998 *Phys. Rev. A* **57** 3627

Walls F L and Dunn G H 1974 *J. Geophys. Res.* **79** 1911